

Article

The Quadratic Local Variance Gamma Model: an arbitrage-free interpolation of class C^3 for option prices

Fabien Le Floc'h

fabien@2ipi.com

Abstract: This paper generalizes the local variance gamma model of Carr and Nadtochiy, to a piecewise quadratic local variance function. The formulation encompasses the piecewise linear Bachelier and piecewise linear Black local variance gamma models. The quadratic local variance function results in an arbitrage-free interpolation of class C^3 . The increased smoothness over the piecewise-constant and piecewise-linear representation allows to reduce the number of knots when interpolating raw market quotes, thus providing an interesting alternative to regularization while reducing the computational cost.

Keywords: volatility surface; interpolation; risk-neutral density; arbitrage; quantitative finance; European options

1. Introduction

The financial markets provide option prices for a discrete set of strike prices and maturity dates. In order to price over-the-counter vanilla options with different strikes, or to hedge complex derivatives with vanilla options, it is useful to have a continuous arbitrage-free representation of the option prices, or equivalently of their implied volatilities. For example, the variance swap replication of Carr and Madan consists in integrating a specific function over a continuum of vanilla put and call option prices [Carr and Lee 2008, Carr and Madan 2001]. More generally, Breeden and Litzenberger [1978] have shown that any path-independent claim can be valued by integrating over the probability density implied by market option prices. An arbitrage-free representation is also particularly important for the Dupire local volatility model [Dupire 1994], where arbitrage will translate to a negative local variance. A option price representation of class C^2 is also key to guarantee the second-order convergence of numerical schemes applied to the Dupire partial differential equation, commonly used to price exotic financial derivative contracts.

A rudimentary, but popular representation is to interpolate market implied volatilities with a cubic spline across option strikes. Unfortunately this may not be arbitrage-free as it does not preserve the convexity of option prices in general. A typical convex interpolation of the call option prices by quadratic splines or rational splines is also not satisfactory in general since it may generate unrealistic oscillations in the corresponding implied volatilities, as evidenced in [Jäckel 2014]. Kahalé [2004] designs an arbitrage-free interpolation of the call option prices, which however requires convex input quotes, employs two embedded non-linear minimizations, and it is not proven that the algorithm for the interpolation function of class C^2 converges.

More recently, Andreasen and Huge [2011] have proposed to calibrate the discrete piecewise constant local volatility corresponding to a single-step finite difference discretization of the forward Dupire equation. In their representation of the local volatility, the authors use as many constants as the number of market option strikes for an optimal fit. It is thus sometimes considered to be "non-parametric". Their technique works well in general but requires some care around the choice of discretization grid: it must be sufficiently dense so that two market strikes do not fall in between the same consecutive grid nodes, and sufficiently wide to properly model the boundary behaviour. Those two requirements complicate, and slow down the non-linear optimization involved in the technique. Furthermore the output is a discrete set of option prices, which, while relatively dense, must still be interpolated carefully to obtain the price of options whose strike falls in between grid nodes.

Le Floc'h and Oosterlee [2019b] derived a specific B-spline collocation to fit the market option prices, while ensuring the arbitrage-free property at the same time. While the fit is quite good in general, it may not

be applicable to interpolate the original quotes with high accuracy. For example, input quotes may already be smoothed out if they stem from a prior model, or from a market data broker, or from another system in the bank. In those cases, it is desirable to use a nearly exact interpolation.

[Le Floc'h \[2021\]](#) extends the local variance gamma model of [Carr and Nadtochiy \[2017\]](#), which relies on a piecewise-constant representation of the local variance function, to a piecewise-linear Bachelier representation. This paper generalizes the model to a piecewise-quadratic function. It encompasses the piecewise-linear Bachelier and piecewise-linear Black representations. The full piecewise-quadratic model results in an arbitrage-free interpolation of class \mathcal{C}^3 for the option prices. The smoother implied probability density allows for the use of a sparser set of interpolation knots, thus providing an alternative to regularization in order to avoid overfitting. In addition, a sparser set of knots reduces the computational cost of the technique.

2. Dupire's PDDE in the local variance gamma model

We recall Dupire's partial difference differential equation (PDDE) for a call option price $C(T, x)$ of strike x and maturity T [[Carr and Nadtochiy 2017](#)]:

$$\frac{C(T, x) - \max(X(0) - x, 0)}{T} = \frac{1}{2} a^2(x) \frac{\partial^2 C(T, x)}{\partial x^2}, \quad (1)$$

for a Martingale asset price process $X(t)$ of expectation $\mathbb{E}_{\mathbb{Q}}[X(t)] = X(0)$. $X(t)$ is driftless, and may thus be the the time T -forward value of a stock price, a foreign exchange rate or a commodity price at time t .

Let $\{x_0, x_1, \dots, x_m, x_{m+1}\}$ be a increasing set of the strike prices, such that $x_0 = L$, $x_{m+1} = U$ with the interval (L, U) being the spatial interval where the asset X lives. Furthermore, we require the following to hold

$$\exists s \in [1, m] \mid x_s = X(0).$$

The (x_1, \dots, x_m) may correspond to the strike prices of the options of maturity T we want to calibrate against, along with the forward price as in [[Carr and Nadtochiy 2017](#), [Le Floc'h 2021](#)]. This choice allows for a nearly exact fit. It may also be some specific discretization of size m with m lower or equal to the number of market strike prices.

We consider a to be a piecewise-quadratic function of class \mathcal{C}^0 on $[x_0, x_m]$.

Let V be the function defined by $V(x) = C(T, x) - \max(X(0) - x, 0)$. V is effectively the time-value¹ of the option. That is, if the option is out-of-the-money (OTM), then $V(x)$ is the option value. If the option is in-the-money (ITM), then $V(x)$ is the option value minus the intrinsic value. The Dupire PDDE leads to

$$V(x) = \frac{1}{2} a^2(x) T [V''(x) + \delta(x - X(0))], \quad (2)$$

on the interval (L, U) , where δ is the Dirac delta function. Instead of solving Equation 2 directly, we look for a solution V on the two intervals $(L, X(0))$ and $(X(0), U)$ separately. On each interval, we have

$$V(x) = \frac{1}{2} a^2(x) T V''(x), \quad (3)$$

Then, the continuity of $\frac{\partial C}{\partial x}$ at $x = X(0)$ implies

$$\lim_{x \rightarrow X(0)^-} V'(x) = 1 + \lim_{x \rightarrow X(0)^+} V'(x). \quad (4)$$

¹ We consider undiscounted option prices.

In order to define a unique V , we also impose the absorbing boundary conditions

$$V(L) = 0 = V(U). \quad (5)$$

The assumption is that the option value is zero for OTM and the intrinsic value for ITM. For these conditions to be plausible, it must be that L and U are far below and above, respectively, the maturity forward price.

The continuity of the second derivative of the call option price $C(T, x)$ at $x = X(0)$ follows from the continuity of $a(x)$ everywhere, including $x = X(0)$ as per [Carr and Nadtochiy \[2017\]](#), Theorem 3.3]. We may further impose a \mathcal{C}^1 continuity of the probability density of X on (L, U) , or equivalently a \mathcal{C}^3 continuity of the option prices C . This requires $a(x)$ to be \mathcal{C}^1 on $(L, X(0))$ and $(X(0), U)$ along with the following continuity condition at $x = x_s$:

$$\lim_{x \rightarrow X(0)-} \left(\frac{V}{a^2} \right)'(x) = \lim_{x \rightarrow X(0)+} \left(\frac{V}{a^2} \right)'(x). \quad (6)$$

Note that $a'(x)$ is not necessarily continuous, and actually should not be continuous for C to be \mathcal{C}^3 . In particular when $a(x) = 1$, C is not \mathcal{C}^3 , because we can not impose Equation 6, given that it would contradict Equation 4.

3. Explicit solution

Let $a(x) = \alpha_i x^2 + \beta_i x + \gamma_i$ on $[x_i, x_{i+1})$ with $(\alpha_i, \beta_i, \gamma_i) \in \mathbb{R}^3$. Being a quadratic, a may also be expressed as $a(x) = \alpha_i(x - \tilde{x}_{i,1})(x - \tilde{x}_{i,2})$ with

$$\tilde{x}_{i,1} = \frac{-\beta_i + \sqrt{\delta_i}}{2\alpha_i}, \quad \tilde{x}_{i,2} = \frac{-\beta_i - \sqrt{\delta_i}}{2\alpha_i}, \quad \text{with } \delta_i = \beta_i^2 - 4\alpha_i\gamma_i, \quad \text{for } \alpha_i \neq 0.$$

In particular, $\tilde{x}_{i,1}$ and $\tilde{x}_{i,2}$ may be complex numbers. When $\alpha_i = 0$ and $\beta_i \neq 0$, we may define $\delta_i = \beta_i^2$ and we have $a(x) = \beta_i(x - \tilde{x}_{i,1})$ with $\tilde{x}_{i,1} = -\gamma_i/\beta_i$.

The solutions of Equation 3 on $[x_i, x_{i+1})$ read

$$V(x) = \frac{\chi_i(x)}{\chi_i(x_i)} \left[\Theta_i^c \cosh(\omega_i(z_i(x) - z_i(x_i))) + \Theta_i^s \sinh(\omega_i(z_i(x) - z_i(x_i))) \right], \quad (7)$$

with²

$$\begin{aligned} z_i(x) &= \ln \left(\frac{x - \tilde{x}_{i,1}}{x - \tilde{x}_{i,2}} \right), & \omega_i &= \frac{1}{2} \sqrt{1 + \frac{8}{\delta_i T}}, & \chi_i &= \sqrt{(x - \tilde{x}_{i,1})(x - \tilde{x}_{i,2})}, & \text{for } \alpha_i \neq 0, \\ z_i(x) &= \ln |x - \tilde{x}_{i,1}|, & \omega_i &= \frac{1}{2} \sqrt{1 + \frac{8}{\delta_i T}}, & \chi_i &= \sqrt{|x - \tilde{x}_{i,1}|}, & \text{for } \alpha_i = 0, \text{ and } \beta_i \neq 0, \\ z_i(x) &= x, & \omega_i &= \frac{1}{\gamma_i} \sqrt{\frac{2}{T}}, & \chi_i &= 1, & \text{for } \alpha_i = 0, \text{ and } \beta_i = 0. \end{aligned}$$

where $(\Theta_i^c, \Theta_i^s) \in \mathbb{C}^2$. The normalization makes $V(x_i) = \Theta_i^c$.

The derivative of V reads

$$V'(x) = \frac{\chi_i(x)}{\chi_i(x_i)} z'_i(x) \left[(\kappa_i \Theta_i^c + \omega_i \Theta_i^s) \cosh(\omega_i(z_i(x) - z_i(x_i))) + (\kappa_i \Theta_i^s + \omega_i \Theta_i^c) \sinh(\omega_i(z_i(x) - z_i(x_i))) \right], \quad (8)$$

² See Appendix A on how to avoid the use of complex numbers.

with

$$\begin{aligned} z'_i(x) &= \frac{1}{x - \tilde{x}_{i,1}} - \frac{1}{x - \tilde{x}_{i,2}}, & \kappa_i &= \frac{1}{2z'_i(x)} \left(\frac{1}{x - \tilde{x}_{i,1}} + \frac{1}{x - \tilde{x}_{i,2}} \right), & \text{for } \alpha_i \neq 0, \\ z'_i(x) &= \frac{1}{x - \tilde{x}_{i,1}}, & \kappa_i &= \frac{1}{2}, & \text{for } \alpha_i = 0 \text{ and } \beta_i \neq 0, \\ z'_i(x) &= 1, & \kappa_i &= 0, & \text{for } \alpha_i = 0 \text{ and } \beta_i = 0. \end{aligned}$$

The conditions to impose continuity of V and its derivative at $x = x_{i+1}$ results in the following linear system

$$\cosh_i \Theta_i^c + \sinh_i \Theta_i^s = \frac{\Theta_{i+1}^c}{\chi_i(x_{i+1})}, \quad (9)$$

$$(\kappa_i \cosh_i + \omega_i \sinh_i) \Theta_i^c + (\omega_i \cosh_i + \kappa_i \sinh_i) \Theta_i^s = \frac{(\kappa_{i+1} \Theta_{i+1}^c + \omega_{i+1} \Theta_{i+1}^s) z'_{i+1}(x_{i+1})}{\chi_i(x_{i+1}) z'_i(x_{i+1})} \quad (10)$$

for $i = 0, \dots, s-2$, with

$$\cosh_i = \cosh(\omega_i(z_i(x_{i+1}) - z_i(x_i))), \quad \sinh_i = \sinh(\omega_i(z_i(x_{i+1}) - z_i(x_i))).$$

The boundary condition at $x = x_0 = L$ translates to $\Theta_0^c = 0$. At $x = x_{m+1} = U$, the boundary condition translates to $\Theta_m^c = -\Theta_m^s \frac{\sinh_m}{\cosh_m}$. The jump condition at $x = s$ reads

$$\begin{aligned} V_{s-1}(x_s) &= V_s(x_s), \\ V'_{s-1}(x_s) &= 1 + V'_s(x_s), \end{aligned}$$

with

$$\begin{aligned} V_{s-1}(x_s) &= \chi_{s-1}(x_s)(\Theta_{s-1}^c \cosh_{s-1} + \Theta_{s-1}^s \sinh_{s-1}), \\ V_s(x_s) &= \Theta_s^c, \\ V'_{s-1}(x_s) &= \chi_{s-1}(x_s) z'_{s-1}(x_s) [(\kappa_{s-1} \Theta_{s-1}^c + \omega_{s-1} \Theta_{s-1}^s) \cosh_{s-1} + (\omega_{s-1} \Theta_{s-1}^c + \kappa_{s-1} \Theta_{s-1}^s) \sinh_{s-1}], \\ V'_s(x_s) &= (\kappa_s \Theta_s^c + \omega_s \Theta_s^s) z'_s(x_s). \end{aligned}$$

From the above equations, we deduce that the coefficients Θ_i^c, Θ_i^s are solutions of the following tridiagonal system³

$$\begin{pmatrix} B_0 & C_0 & & 0 \\ A_1 & \ddots & \ddots & \\ & \ddots & \ddots & C_{2m} \\ 0 & & A_{2m+1} & B_{2m+1} \end{pmatrix} \begin{pmatrix} \Theta_0^s \\ \Theta_0^c \\ \vdots \\ \Theta_m^s \\ \Theta_m^c \end{pmatrix} = \begin{pmatrix} D_0 \\ \vdots \\ D_{2m+1} \end{pmatrix}, \quad (11)$$

³ the A, B and C of the tridiagonal matrix are not known a-priori. In the case of a quadratic B-spline representation, they will be a function of the B-spline parameters λ . The value λ will be determined by a least squares minimization of the error between model prices and market prices. One step in the least-squares objective function is to solve the (then known) tridiagonal system.

with $D_i = 0$ for $i \notin \{2s-1, 2s\}$, $D_{2s-1} = D_{2s} = 1$,

$$\begin{cases} A_{2i+1} = (\omega_i \cosh_i + \kappa_i \sinh_i) \chi_i z'_i(x_{i+1}) - \kappa_{i+1} \sinh_i \chi_i z'_{i+1}(x_{i+1}), \\ B_{2i+1} = (\kappa_i \cosh_i + \omega_i \sinh_i) \chi_i z'_i(x_{i+1}) - \kappa_{i+1} \cosh_i \chi_i z'_{i+1}(x_{i+1}), \\ C_{2i+1} = -\omega_{i+1} z'_{i+1}(x_{i+1}), \\ A_{2i+2} = \left(\kappa_i \cosh_i + \omega_i \sinh_i - \frac{\omega_i \cosh_i + \kappa_i \sinh_i}{\sinh_i} \cosh_i \right) \chi_i z'_i(x_{i+1}), \\ B_{2i+2} = -\omega_{i+1} z'_{i+1}(x_{i+1}), \\ C_{2i+2} = \frac{\omega_i \cosh_i + \kappa_i \sinh_i}{\sinh_i} z'_i(x_{i+1}) - \kappa_{i+2} z'_{i+1}(x_{i+1}), \end{cases}$$

for $i = 0, \dots, m-1$, and $B_0 = 0, C_0 = 1, A_{2m+1} = \sinh_m, B_{2m+1} = \cosh_m$.

Using the continuity of $V(x_s) = \Theta_s^c$, the jump condition of V' at x_s and the continuity of $a(x_s)$, the \mathcal{C}^3 condition (Equation 6) reads

$$1 - 2\Theta_s^c \frac{\lim_{x \rightarrow x_s^-} a'(x)}{a(x_s)} = -2\Theta_s^c \frac{\lim_{x \rightarrow x_s^+} a'(x)}{a(x_s)}. \quad (12)$$

Equation 12 implies that a' is not continuous at x_s , unless $a(x_s) = 0$. The condition can not be imposed as an additional constraint on Θ_s^c since its value is already fully determined by the tridiagonal system. It may however be imposed by choosing the correct model parameter to adjust the value of a at x_s along with its left and right derivative values.

4. Parameterizations

4.1. Linear Bachelier

The linear Bachelier local variance consists in $\alpha_i = 0$ and may be rewritten using values at the knots σ_i as

$$a(x) = \frac{x - x_i}{x_{i+1} - x_i} (\sigma_{i+1} - \sigma_i) + \sigma_i \quad \text{for } x_i \leq x < x_{i+1}, \quad i = 0, \dots, m, \quad (13)$$

where the parameters $\sigma_i > 0$.

It corresponds to the parameterization studied in [Le Floch 2021], where it is shown that the local variance function must not be \mathcal{C}^1 at $x = x_s$ but must follow \mathcal{C}^3 condition (Equation 12) in order to avoid a spurious spike at $x = x_s$. Under the linear Bachelier local variance, the condition reads

$$1 - 2\Theta_s^c \frac{\sigma_s - \sigma_{s-1}}{(x_s - x_{s-1})\sigma_s} = -2\Theta_s^c \frac{\sigma_{s+1} - \sigma_s}{(x_{s+1} - x_s)\sigma_s},$$

or equivalently

$$\sigma_s = \frac{2\Theta_s^c \left(\frac{\sigma_{s-1}}{x_s - x_{s-1}} + \frac{\sigma_{s+1}}{x_{s+1} - x_s} \right)}{2\Theta_s^c \left(\frac{1}{x_s - x_{s-1}} + \frac{1}{x_{s+1} - x_s} \right) - 1}. \quad (14)$$

This is not a linear problem, as Θ_s^c depends on σ_s through $\Theta_{s+1}^c, \Theta_{s+1}^s$ in a non-linear way (Equations 9 and 10). Starting with the algorithm described in Section 3 to compute Θ^c, Θ^s , using Equation 14 with $\Theta_s^c \approx V_{\text{market}}(x_s)$ as initial guess for σ_s , we may however apply the following iteration

- Update σ_s through Equation 14.
- Recalculate Θ_i^c and Θ_i^s for $i = 0, \dots, m$ by solving the updated tridiagonal system.

Three iterations are enough in practice. It may happen that the denominator of the right hand side of Equation 14 is negative when the distances $x_{s+1} - x_s$ and $x_s - x_{s-1}$ are large. We found it sufficient to move x_{s+1} and x_{s-1} such that the denominator is guaranteed⁴ to be positive for the initial guess.

4.2. Linear Black

The linear Black local variance model is defined by $\gamma = 0$. The local variance function may be rewritten using values at the knots σ_i as

$$a(x) = \left(\frac{x - x_i}{x_{i+1} - x_i} (\sigma_{i+1} - \sigma_i) + \sigma_i \right) x \quad \text{for } x_i \leq x < x_{i+1}, \quad i = 0, \dots, m, \quad (15)$$

where the parameters $\sigma_i > 0$. Interestingly, the \mathcal{C}^3 condition (Equation 12) is also given by Equation 14.

4.3. Positive quadratic B-spline

A B-spline parameterization with positive coefficients implies a positive. Furthermore, Equation 12 imposes a double knot at $x = x_s$ (because the derivative of a is not continuous there). We thus consider

$$a(x) = \sum_{i=1}^{m+3} \lambda_i B_{i,3}(x) \quad (16)$$

where $\lambda_i > 0$ and $B_{i,3}$ is the quadratic basis spline with knots $t = (L, L, L, x_1, x_2, \dots, X(0), X(0), \dots, x_m, U, U, U)$. In particular, we have $t_{s+2} = t_{s+3} = X(0)$. Using the B-spline derivative identity [De Boor 1978] and the fact that the order of the B-spline is 3, we obtain

$$a'(x) = 2 \sum_i \frac{\lambda_i - \lambda_{i-1}}{t_{i+2} - t_i} B_{i-1,2}(x),$$

and the \mathcal{C}^3 condition reads

$$\sum_i \lambda_i B_{i,3}(x_s) = 4\Theta_s^c \left(\frac{\lambda_{s+1} - \lambda_s}{t_{s+3} - t_{s+1}} B_{s,2}(x_s^-) - \frac{\lambda_{s+2} - \lambda_{s+1}}{t_{s+4} - t_{s+2}} B_{s+1,2}(x_s^+) \right).$$

Using the definitions of $B_{i,3}$ and $B_{i,2}$ we obtain

$$\lambda_{s+1} = 4\Theta_s^c \left(\frac{\lambda_{s+1} - \lambda_s}{t_{s+3} - t_{s+1}} - \frac{\lambda_{s+2} - \lambda_{s+1}}{t_{s+4} - t_{s+2}} \right),$$

or equivalently

$$\lambda_{s+1} = \frac{4\Theta_s^c \left(\frac{\lambda_s}{t_{s+3} - t_{s+1}} + \frac{\lambda_{s+2}}{t_{s+4} - t_{s+2}} \right)}{4\Theta_s^c \left(\frac{1}{t_{s+3} - t_{s+1}} + \frac{1}{t_{s+4} - t_{s+2}} \right) - 1}. \quad (17)$$

⁴ We pick $h = \min(x_{s+1} - x_s, x_s - x_{s-1}, 3V_{\text{market}}(x_s))$ and set the new $x_{s+1} = x_s + h$ $x_{s-1} = x_s - h$.

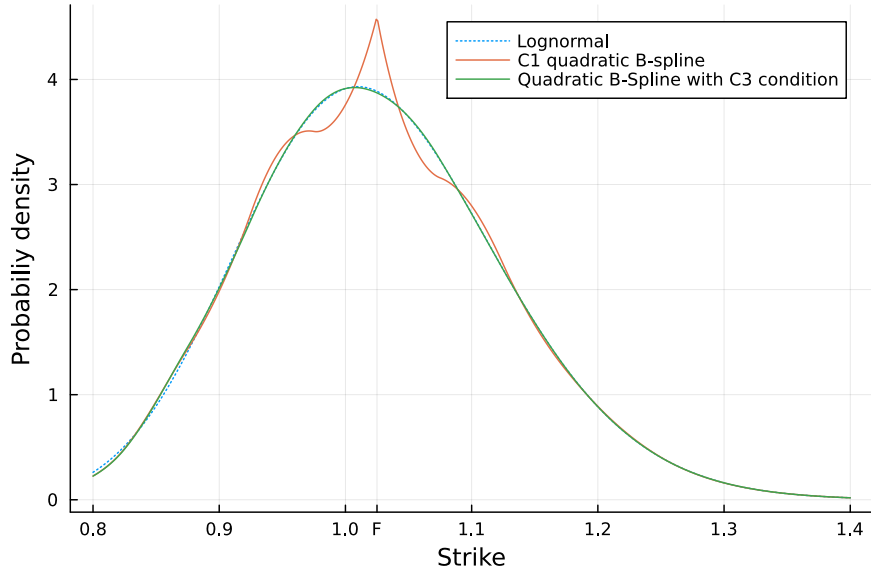


Figure 1. Implied probability density for the quadratic LVG model with or without the \mathcal{C}^3 condition (Equation 6), fitted to a Black-Scholes model with constant volatility $\sigma_B = 20\%$, time to expiry $T = 0.25$ and forward 1.025.

As an illustration, we consider the same example as in [Le Floc'h 2021]: we fit the quadratic local variance gamma (LVG) model to 10 option prices of strikes (0.85, 0.90, 0.95, 1, 1.05, 1.1, 1.15, 1.2, 1.3, 1.4), obtained by the Black-Scholes model with constant volatility $\sigma_B = 20\%$, time to maturity $T = 0.25$ and forward price 1.025. We know that the theoretical distribution is a lognormal distribution. A straightforward \mathcal{C}^1 quadratic B-spline leads to a large spike in the probability density implied from the calibrated LVG model (Figure 1). Adding the \mathcal{C}^3 condition through an additional B-spline knot recovers a smooth implied probability density.

5. Calibration

5.1. Error measure

The calibration of a single maturity consists in finding the parameters (the α for the linear models, or λ for the quadratic B-spline) such that the function $C(T, x)$, solution of the Dupire PDDE fits the market option prices $(\hat{C}_i)_{i=1,\dots,n}$ of respective strikes $(K_i)_{i=1,\dots,n}$ according to an appropriate measure. A common practice is to perform a least-squares minimization of the error measure E defined by

$$E = \sum_{i=1}^m \mu_i^2 (\sigma(\alpha, x_i) - \hat{\sigma}_i)^2, \quad (18)$$

with $\alpha_i > 0$ for $i = 1, \dots, m$ and where $\sigma(\alpha, x)$ is the implied volatility corresponding to the option prices obtained with the piecewise-linear local gamma variance model and $\hat{\sigma}_i$ is the market implied volatility at strike x_i , $(\mu_i)_{i=1,\dots,m}$ are weights associated to the accuracy of the fit at each point.

In order to solve this non-linear least-squares problem, we will use the Levenberg-Marquardt algorithm as implemented by [Klare and Miller \[2013\]](#). The box constraints $\alpha_i > 0$ can be added in a relatively straightforward manner to any Levenberg-Marquardt algorithm, through the projection technique described in [\[Kanzow et al. 2004\]](#), or through a variable transform from \mathbb{R} to a subset of \mathbb{R}^+ (for example through the function $x \rightarrow x^2 + \epsilon$ with some small positive ϵ).

The implied volatility for a given option price may be found efficiently and accurately through the algorithm of [Jäckel \[2015\]](#). In general, we prefer to solve an almost equivalent formulation in terms of option prices, using the error measure E_V defined by

$$E_V = \sum_{i=1}^m w_i^2 (C(\alpha, x_i) - \hat{C}_i)^2, \quad (19)$$

with $C(\alpha, x)$ being the local variance gamma option price with parameter α and strike x , and the capped inverse Vega weights w_i given by

$$w_i = \min\left(\frac{1}{\nu_i}, \frac{10^6}{X(0)}\right) \mu_i, \quad (20)$$

where $\nu_i = \frac{\partial \hat{C}_i}{\partial \sigma}$ is the Black-Scholes Vega corresponding the market option price \hat{C}_i , and 10^6 is a cap applied to avoid numerical issues related to the limited machine accuracy (see [Le Floc'h \[2021\]](#), [Le Floc'h and Oosterlee \[2019b\]](#) for the justification).

5.2. Exact interpolation

Sometimes, it is desirable to interpolate a given set of reference prices nearly exactly. This is typically the case when the reference prices come from some prior model. We apply the same least-square minimization but choose the number of free parameters to be equal to the number of reference prices.

5.2.1. Linear models

For the linear models, this means to use $m = n$ and set $\alpha_0 = \alpha_1$ and $\alpha_{m+1} = \alpha_m$ to model a flat extrapolation. In general, the market strikes will not include $X(0)$. In this case, $X(0)$ must be added to the knots $\{x_i\}_{i=1,\dots,m}$ used in the local variance gamma representation. This adds one more parameter α_s to the representation, where s is the index corresponding to $X(0)$ in the set of knots. The value of α_s is not free, it is given by the \mathcal{C}^3 condition (Equation 6) and enforced through the iterative procedure described in the previous sections.

5.2.2. B-spline knots locations

For the linear Bachelier and Black parameterization, choosing the knots at the market strikes works well. The situation is more complex for the quadratic B-spline parameterization.

Let $(K_i)_{i=1,\dots,n}$ be the market options strikes. Let the index i_F be such that $K_{i_F} \leq F < K_{i_F+1}$. We may:

- place the knots at the market strikes (labeled "Strikes" in the figures)

$$t = \begin{cases} (L, L, L, K_1, \dots, K_{i_F}, F, F, K_{i_F+1}, \dots, K_n, U, U, U) & \text{if } K_{i_F} \neq F \\ (L, L, L, K_1, \dots, K_{i_F}, F, K_{i_F+1}, \dots, K_n, U, U, U) & \text{if } K_{i_F} = F \end{cases},$$

The dimension of λ is then $n_\lambda = n + 5$ if $F \neq K_{i_F}$ and $n + 4$ if $F = K_{i_F}$. The change in the number of dimensions suggests that the interpolation may change significantly when the forward price moves across a market strike.

- place the knots in the middle of market strikes. According to [\[De Boor 1978, p. 61\]](#), the \mathcal{C}^1 quadratic spline is then solution to a diagonally dominant tridiagonal system, which increases the stability and reduce oscillations of the interpolation. There are however several ways to do it:

- choose the direct mid-points (labeled "Mid-Strikes")

$$t = \begin{cases} \left(L, L, L, \frac{K_1+K_2}{2}, \dots, \frac{K_{i_F-1}+K_{i_F}}{2}, F, F, \frac{K_{i_F}+K_{i_F+1}}{2}, \dots, \frac{K_{n-1}+K_n}{2}, U, U, U\right) & \text{if } F < \frac{K_{i_F}+K_{i_F+1}}{2} \\ \left(L, L, L, \frac{K_1+K_2}{2}, \dots, \frac{K_{i_F-1}+K_{i_F}}{2}, \frac{K_{i_F}+K_{i_F+1}}{2}, F, F, \dots, \frac{K_{n-1}+K_n}{2}, U, U, U\right) & \text{if } F > \frac{K_{i_F}+K_{i_F+1}}{2} \\ \left(L, L, L, \frac{K_1+K_2}{2}, \dots, \frac{K_{i_F-1}+K_{i_F}}{2}, F, F, \frac{K_{i_F+1}+K_{i_F+2}}{2}, \dots, \frac{K_{n-1}+K_n}{2}, U, U, U\right) & \text{if } F = \frac{K_{i_F}+K_{i_F+1}}{2} \end{cases},$$

The dimension of λ is then $n_\lambda = n + 4$ if $F \neq K_{i_F}$ and $n + 3$ if $F = K_{i_F}$.

- choose the mid-points, excluding the point closest to the forward price F (labeled "Mid-X")

$$t = \left(L, L, L, \frac{K_1 + K_2}{2}, \dots, \frac{K_{i_F-1} + K_{i_F}}{2}, F, F, \frac{K_{i_F+1} + K_{i_F+2}}{2}, \dots, \frac{K_{n-1} + K_n}{2}, U, U, U \right),$$

The dimension of λ is then $n_\lambda = n + 3$.

- choose the mid-points, excluding the point closest to the forward price and placing the first and last strike in the middle of two knots (labeled "Mid-XX")

$$t = \left(L, L, L, \frac{3K_1 - K_2}{2}, \frac{K_1 + K_2}{2}, \dots, \frac{K_{i_F-1} + K_{i_F}}{2}, F, F, \frac{K_{i_F+1} + K_{i_F+2}}{2}, \dots, \frac{K_{n-1} + K_n}{2}, \frac{3K_n - K_{n-1}}{2}, U, U, U \right),$$

The dimension of λ is then $n_\lambda = n + 5$.

- use a uniform discretization of $[K_1, K_n]$ composed of $n + 1$ points, and shift it such that the forward is exactly part of the knots and we have $n_\lambda = n + 5$.

In each of those case, we make sure to add the forward price as a double knot, as well as the boundaries L, U . The dimension of λ implied by the knots is larger than the number of market strikes. We choose the extra parameters as such:

- if $n_\lambda = n + 5$, we set $\lambda_1 = \lambda_2 = \lambda_3$, $\lambda_{n+3} = \lambda_{n+4} = \lambda_{n+5}$ and λ_{i_F+3} is obtained from λ_{i_F+2} and λ_{i_F+4} .
- if $n_\lambda = n + 4$, we set $\lambda_1 = \lambda_2 = \lambda_3$, $\lambda_{n+3} = \lambda_{n+4}$ and λ_{i_F+3} is obtained from λ_{i_F+2} and λ_{i_F+4} .
- if $n_\lambda = n + 3$, we set $\lambda_1 = \lambda_2$, $\lambda_{n+2} = \lambda_{n+3}$ and λ_{i_F+2} is obtained from λ_{i_F+1} and λ_{i_F+3} .

In order to assess the various knots candidates, we consider the same example as in the previous section, but using a few different random sets of 10 strikes in the interval $[85, 140]$ and a forward price $F = 101$ (Table 1).

Table 1. Sets of market strikes with a Black-Scholes volatility of 20% for a maturity $T = 0.25$ and forward $F = 101$.

| Set | K_1 | K_2 | K_3 | K_4 | K_5 | K_6 | K_7 | K_8 | K_9 | K_{10} |
|-----|-------|--------|--------|--------|--------|--------|--------|--------|--------|----------|
| A | 88.77 | 92.85 | 93.38 | 99.37 | 107.99 | 120.29 | 122.03 | 123.9 | 134.71 | 135.43 |
| B | 85.02 | 101.92 | 103.55 | 114.45 | 121.85 | 123.69 | 125.07 | 125.58 | 131.63 | 133.86 |
| C | 98.07 | 100.93 | 101.06 | 106.88 | 109.12 | 110.93 | 119.76 | 119.83 | 132.19 | 138.27 |
| D | 85.00 | 90.00 | 95.00 | 100.00 | 101.00 | 105.00 | 110.00 | 115.00 | 120.00 | 130.00 |

Table 2. Root mean square error in implied volatilities % for various choices of B-spline knots. The reference volatilities are flat 20%.

| Set | Strikes | Mid-Strikes | Mid-X | Mid-XX | Uniform |
|-----|---------|-------------|--------|--------|---------|
| A | 9.4e-8 | 6.0e-3 | 5.2e-3 | 4.1e-8 | 4.8e-9 |
| B | 9.9e-9 | 2.8e-3 | 5.8e-1 | 2.9e-6 | 9.9e-3 |
| C | 1.0e-6 | 1.9e-3 | 1.0e-2 | 1.1e-8 | 1.4e-3 |
| D | 4.1e-4 | 8.1e-2 | 4.1e-2 | 2.6e-5 | 5.0e-7 |

The uniform discretization may⁵ result in strong oscillations due to overfitting in places where no market strike is quoted as in the set A (Figure 2(a)).

⁵ In practice, market strikes are not randomly distributed, but according to multiples of a minimum strike width, with more strikes near the money. The uniform discretization may still be relevant if some regularization is added to the objective of the minimizer.

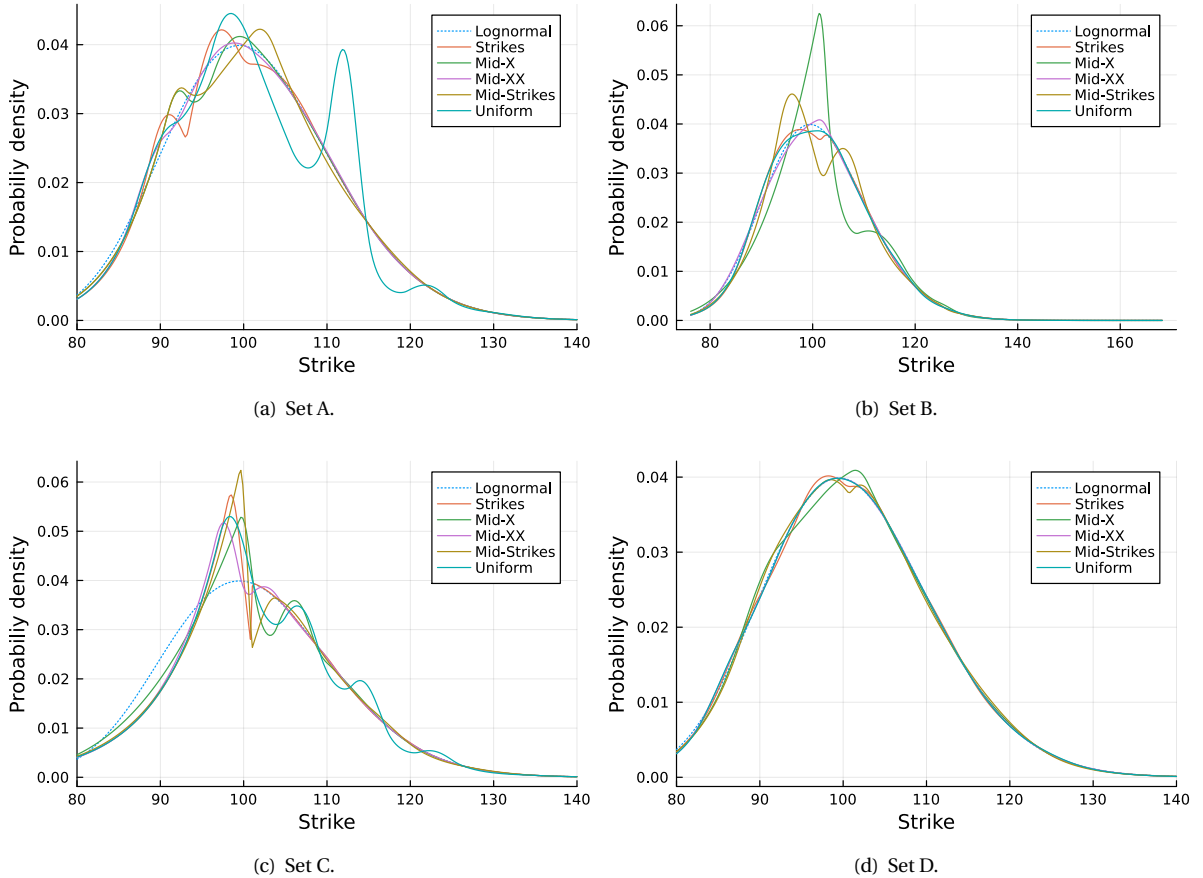


Figure 2. Implied probability density of the calibrated quadratic LVG model using different sets of knots.

The "Mid-Strikes" choice leads to a strong oscillation around the forward in set B (Figure 2(b)). The "Mid-X" produces a somewhat awkward shape on the set B. When the forward is very close to some of the knots as in set C, the "Strikes", "Mid-Strikes" choices lead to a density with a sharp gradient near the forward, a feature not desirable (Figure 2(c)). When the forward is part of the market strikes, a small wiggle is visible at the forward for "Strikes" and "Mid-Strikes" (Figure 2(d)).

Finally it is also interesting to look at the overall root mean square error in implied volatilities for the different choices (Table 2). The "Strikes" and "Mid-XX" choices consistently result in a near-perfect⁶ fit.

Overall, the "Mid-XX" knots lead to the most stable probability density along with an excellent fit.

5.2.3. Many quotes, few parameters

In [Le Floc'h 2021], regularization is employed to ensure a smooth implied probability density when fitting to many, eventually noisy, market option quotes. An interesting simpler alternative is to use few knots/few parameters instead of as many parameters as market quotes: by limiting the number of free-parameters, we may avoid overfitting issues, and at the same time we reduce the number of dimensions of the problem, thus increasing stability and performance. Where to place the knots then? Based on the previous observations, we may choose knots such that the market strikes are equidistributed. Concretely, we use

$$\tilde{K} = \{K_1, K_{1+j}, K_{1+2j}, \dots, K_n\},$$

⁶ The error in volatility is always below one basis point.

where $j = n/m$ with $m \leq n$ and use the "Mid-XX" knots on top of \tilde{K} . It may happen that many market strikes are quoted in a narrow range, in which case the set could be adjusted with a minimum strike width, although we did not need this tweak on the market examples presented below.

We consider previously published examples of real-world implied volatility smiles of equity indices, equities or foreign exchange rates which present interesting characteristics. The first example, presented in Table A1, is the case of SPX500 expiring on March 24, 2017 as March 16, 2017 (one week - 1w) that the SVI parametrization of [Gatheral \[2006\]](#) fails to fit properly.

The second example presented in Table A2 consists in options on SPX500 expiring on March 7, 2018 as of February 5, 2018 (one month - 1m) where the implied volatility smile exhibits a very high curvature, where the polynomial stochastic collocation leads to a somewhat unnatural spike in the probability density while a mixture of lognormals leads to a multimodal implied density [[Le Floc'h and Oosterlee 2019a](#)].

The third example uses very recent option quotes on TSLA of maturity March 21, 2025 as of February 21, 2025 (1m). The reference implied volatilities corresponding to the mid option prices are given in Table A3. The peculiarity of TSLA stock is that the volatility is relatively high. On this example, SVI does not fit the volatilities close to the money very well, while the xSSVI of [Corbetta et al. \[2019\]](#) and SABR from [Hagan et al. \[2002\]](#) (not shown for clarity) would be even worse.

The fourth example shows a W shaped implied volatility, typical before major earning events, for options on AAPL with expiry in 4 days as of October 28, 2013 (4d) from [Alexiou et al. \[2021\]](#). Simple parametric models such as SVI or SABR or even polynomial stochastic collocation are unable to produce this kind of shape.

The fifth example (Table A4) involves options on the AUD/NZD currency pair of maturity July 9, 2014 as of July 2, 2014 (1w) from [Wystup \[2018\]](#), where a typical calibration of SVI leads to a negative implied probability density.

There is an apparent focus on short maturities as those are more difficult to capture, with a variety of smile shapes, with some exhibiting multi-modality. As the implied volatility smile flattens for long maturities, those are much easier to fit to.

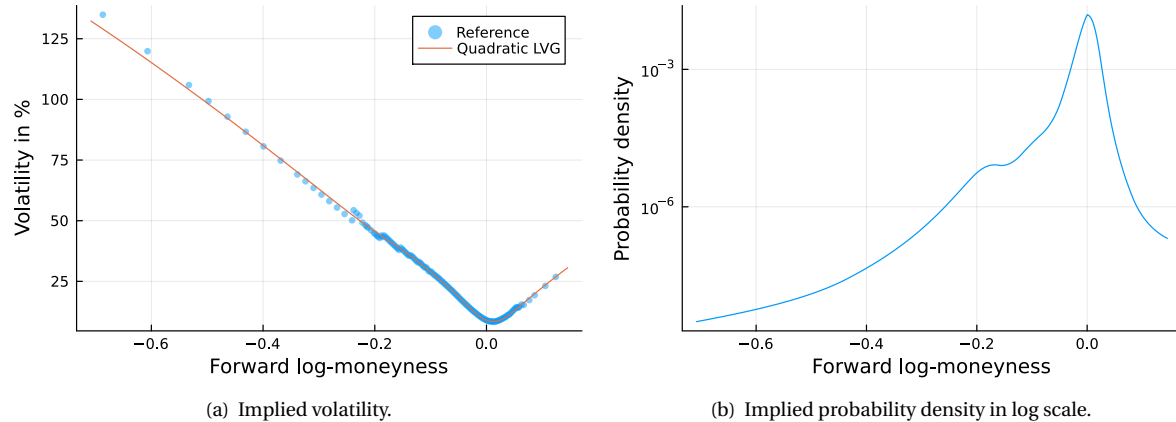


Figure 3. Quadratic LVG model with 10 points calibrated to SPX500 options of maturity 1w.

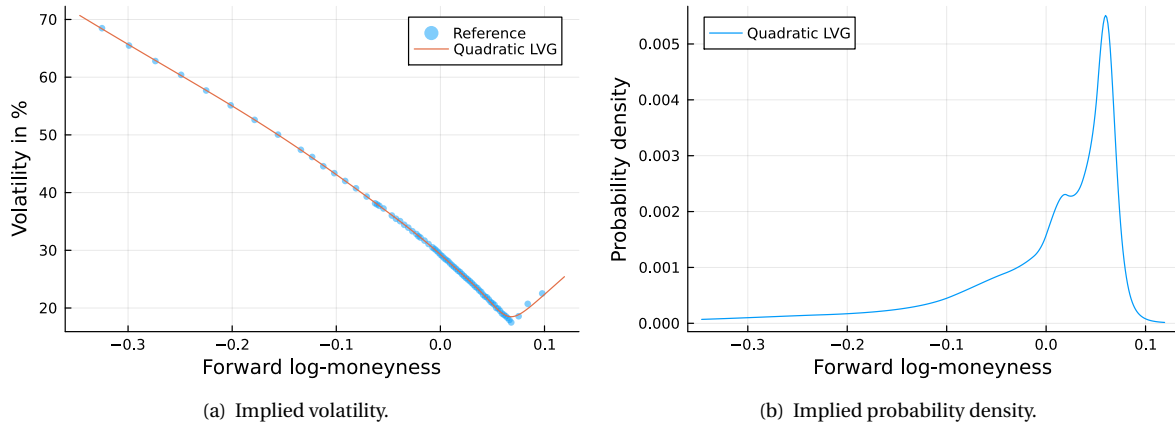


Figure 4. Quadratic LVG model with 10 points calibrated to SPX500 options of maturity 1m.

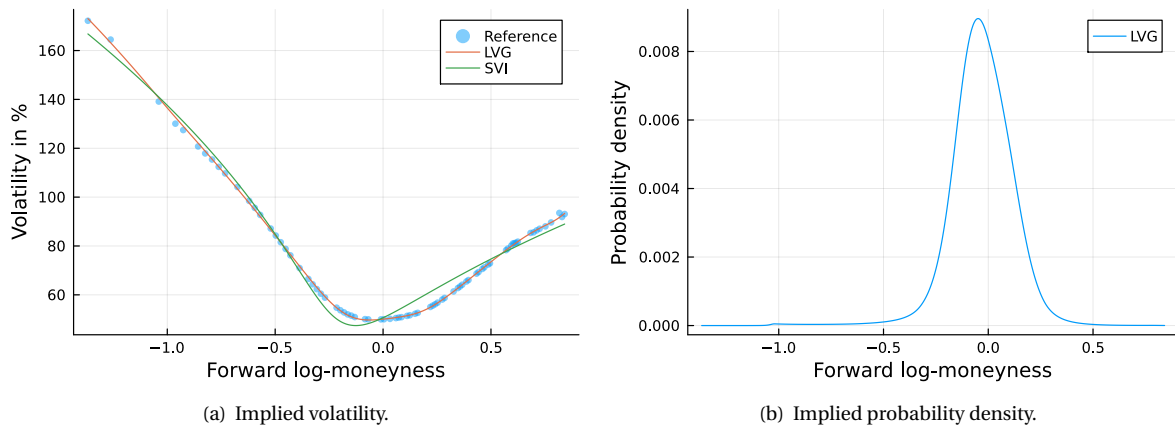


Figure 5. Quadratic LVG model with 10 points calibrated to TSLA options of maturity 1m.

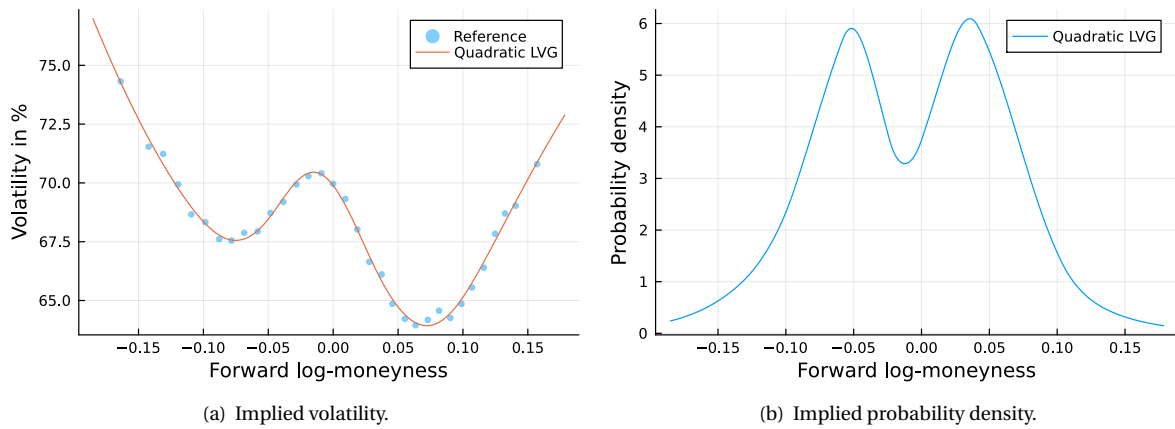


Figure 6. Quadratic LVG model with 10 points calibrated to AAPL options of maturity 4d.

The AUD/NZD foreign exchange smile from [Wystup \[2018\]](#) is useful to see how the local variance gamma model behaves on a minimalistic example: indeed, as is usual on the foreign exchange options market, it involves only five options quotes. In this case we use as many parameters as market quotes. Figure 7(b) shows that the density implied by the quadratic LVG model is smooth, but the one implied by the linear Bachelier LVG model exhibits some sharp unnatural gradients near the money.

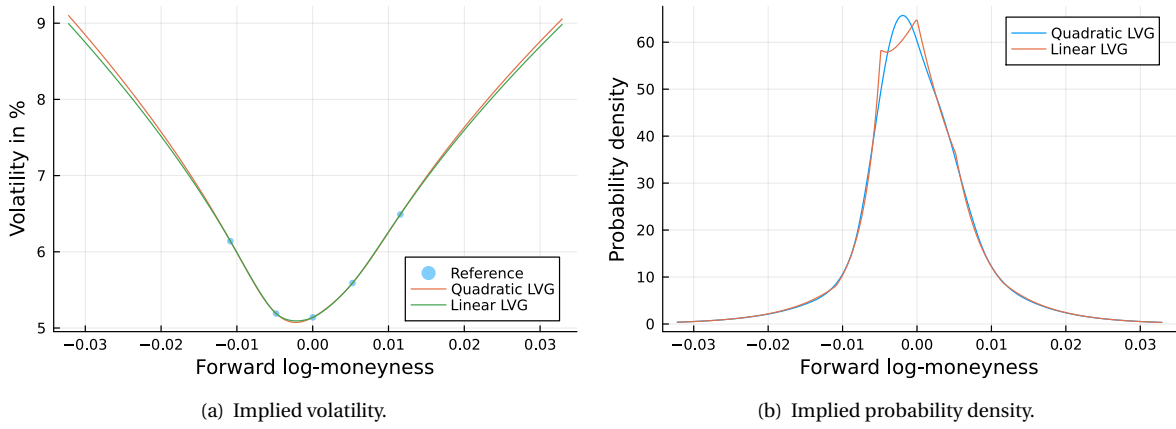


Figure 7. Quadratic LVG model with 5 points calibrated to AUD/NZD options of maturity 1w.

Indeed, the linear LVG model leads only to a \mathcal{C}^0 probability density. Such gradients are then inevitable when the number of quotes is small. On this example, the (unconstrained) SVI model is known to lead to some negative probability density.

In all the examples considered so far, the fit in terms of implied volatilities is excellent, and the implied probability density is smooth, without spurious peaks, although the number of points considered ($n = 10$) is somewhat arbitrary.

5.2.4. Challenging examples of exact interpolation

We consider the manufactured examples of [Jäckel \[2014\]](#) presented in Table A5. In the first example, a cubic spline interpolation of option prices is known to produce oscillations in the implied volatility, while a cubic spline on the volatilities introduces spurious arbitragers. In the second example, some of the quotes are at the limit of arbitrage.

On those examples, some care need to be taken in the choice of the boundaries L and U : they must be far away enough. We pick $L = K_1/2$ and $U = 2K_m$ where K_1 is the smallest quoted strike and K_m the largest.

On the example case I, the fit is nearly exact for the linear Bachelier, Black and quadratic LVG models and there is no oscillation or wiggles in the implied volatility interpolation (Figure 8(a)). The corresponding implied probability density is of course smoothest with the quadratic LVG model (Figure 8(b)).

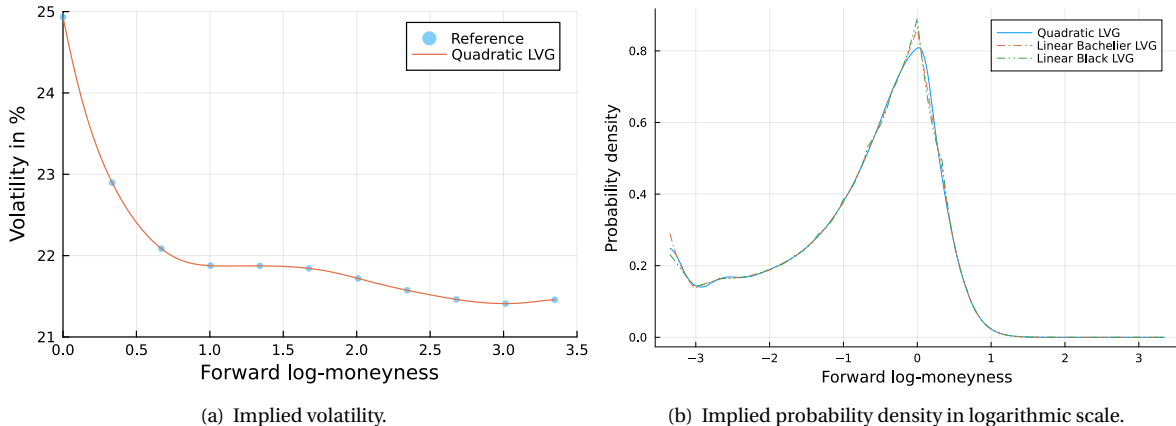


Figure 8. LVG models calibrated to the example case I of [Jäckel \[2014\]](#).

On the example case II, the quadratic LVG model does not allow for an exact fit. The root mean square error is around 4 basis points (Table 3), the fit is qualitatively good (Figure 9(a)). The near-arbitragers impose the probability density to go to almost zero, which conflicts with the \mathcal{C}^1 continuity constraints of

parameterized B-spline density. The density stays however smooth, and looks more natural than the clear overfit of the linear LVG models (Figure 9(b)).

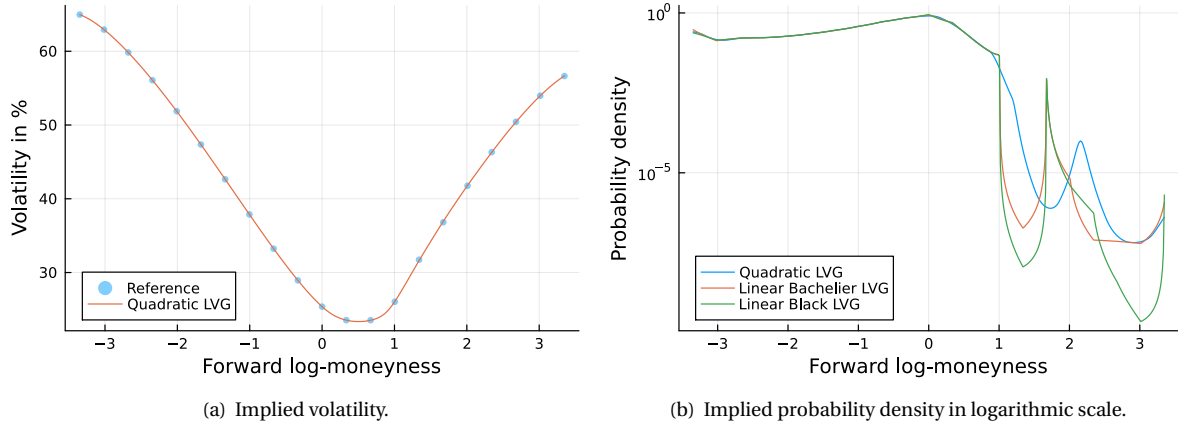


Figure 9. LVG models calibrated to the example case II of Jäckel [2014].

Our choice of range for the α parameter does not allow the linear Bachelier model to fit as well as the linear Black model. Increasing the range would make the two implied probability densities even more similar.

Table 3. Root mean square error (RMSE) in implied volatilities of the LVG models calibrated to the market data of Table A5.

| Model | Case I | Case II |
|------------------|----------|---------|
| Linear Bachelier | 5.00e-13 | 4.54e-6 |
| Linear Black | 3.64e-12 | 8.04e-8 |
| Quadratic | 2.25e-12 | 4.02e-4 |

5.2.5. Multiple maturities - interpolation in time

In order to fit multiple option maturities and obtain a continuous representation of the implied volatility surface in both strikes and expiry time, the simplest approach consists in calibrating each maturity independently and interpolate in between maturities in total variance. While often used by practitioners due to its simplicity, this approach may however introduce calendar spread arbitrages (or equivalently, areas of negative forward variance). A possible work-around is to calibrate from the shortest maturity to the longest, paying attention to eventually shift the reference (market) quotes upwards if the previous maturity leads to a calendar spread with the current maturity to calibrate. This still does not guarantee the absence of calendar spreads in between market strikes, and even at the market strikes if the calibrated prices differ significantly from the market prices.

Another approach, suggested in [Falck and Deryabin 2017], is to make sure the total local variance parameterization increases with the time to maturity. For the B-spline parameterization this requires to

- use the same knots for all the market option maturities. To do so, we divide the prices and strikes by the forward at each maturity and use a forward $F(0, T_i) = 1$ in the LVG calibration. This will provide a natural interpolation across constant forward moneyness. The original option price may be recovered by multiplying the model price by the forward at the relevant maturity. We also choose the "Mid-XX" knots of the first maturity, but we may use any maturity to base our knots on as they do not need to match any market strike.
- ensure that $\lambda_{T_i} > \lambda_{T_{i-1}}$ during the calibration instead of $\lambda_{T_i} > 0$ where λ_{T_i} are the B-spline parameters for the maturity T_i and $T_i > T_{i-1}$. This is guarantees that the total local variance function $a(x)$ increases with the time to maturity for every $x \in [L, U]$, which is a sufficient condition to guarantee the absence of calendar spread arbitrages.

On the example market data of [Kahalé \[2004\]](#), the above calibration method results in smooth implied variance curves. As expected from the absence of calendar spread arbitrages, the curves do not cross in Figure 10. The error in implied volatility is larger for the longer maturities, with up to 6 basis points for the last maturity. This may still be acceptable, and the increased smoothness is attractive. An additional global calibration step where all the expiries are calibrated together, based on the bootstrap calibration as initial guess, would allow to further improve the fit. In between maturities, we may interpolate linearly the B-spline parameters in the square root of time:

$$\lambda_t = \lambda_{T_{i-1}} + (\lambda_{T_i} - \lambda_{T_{i-1}}) \frac{\sqrt{t - T_{i-1}}}{\sqrt{T_i - T_{i-1}}},$$

for $T_{i-1} < t \leq T_i$. The corresponding "flat volatility" extrapolation would consist in using $\lambda_{T_1} \sqrt{t/T_1}$ for $t < T_1$ and $\lambda_{T_N} \sqrt{t/T_N}$ for $t > T_N$. Alternatively we may use a linear interpolation in total variance with flat implied volatility extrapolation. The resulting Dupire local volatility surface is smooth (Figure 11).

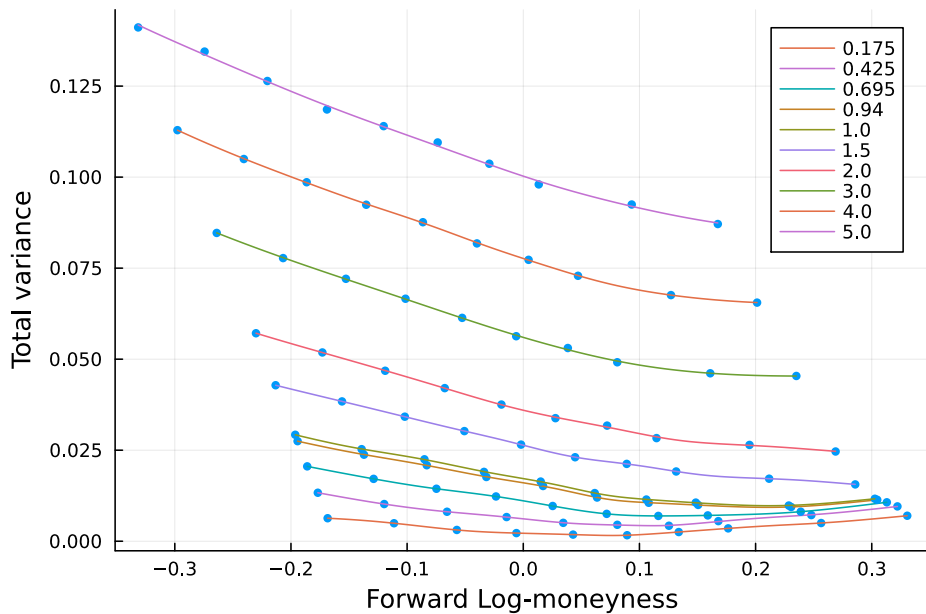


Figure 10. Implied variance from the quadratic LVG model calibrated to the market data of [Kahalé \[2004\]](#).

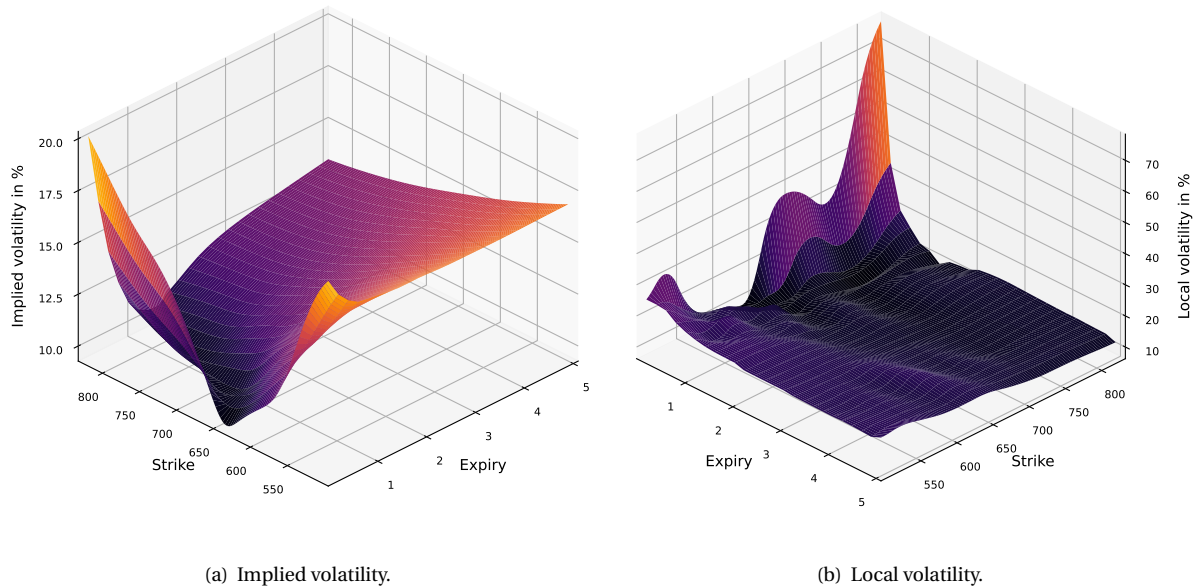


Figure 11. Volatility surfaces from the quadratic LVG model calibrated to the market data of [Kahalé \[2004\]](#).

6. Conclusion

The quadratic local variance gamma model with a small number of knots lead to smooth implied probability densities on a variety of market option quotes, while providing an excellent fit in terms of implied volatilities, even on challenging examples of non convex implied volatilities or multi-modal probability densities.

It thus constitutes an interesting alternative to the non-parametric approaches of the linear or quadratic local variance gamma models or of the Andreasen-Huge one-step local volatility model, which all require a non-trivial choice of regularization constant to produce a smooth implied probability density.

In similar fashion as [Falck and Deryabin \[2017\]](#), it may be used as specific generic parameterization with a fixed, small number of parameters using only 3 or 5 points. In contrast to [Falck and Deryabin \[2017\]](#), where the linear parameterization leads to edges in the implied probability density and where the problem of the discontinuity at the forward is not dealt with, the probability density of the quadratic LVG model with a reduced number of points will be smooth.

Further research may explore the use of Fourier transforms to recover efficient pricing formulae for European options under the local variance gamma model with a more general local variance function.

Alexiou, Lykourgos, Amit Goyal, Alexandros Kostakis, and Leonidas Rompolis. 2021. Pricing event risk: Evidence from concave implied volatility curves. *Swiss Finance Institute Research Paper* (21-48).

Andreasen, Jesper and Brian Huge. 2011. Volatility interpolation. *Risk* 24(3), 76.

Breeden, Douglas T and Robert H Litzenberger. 1978. Prices of state-contingent claims implicit in option prices. *Journal of business*, 621–651.

Carr, Peter and Roger Lee. 2008. Robust replication of volatility derivatives. In *Prmia award for best paper in derivatives, mfa 2008 annual meeting*.

Carr, Peter and Dilip Madan. 2001. Towards a theory of volatility trading. *Option Pricing, Interest Rates and Risk Management, Handbooks in Mathematical Finance*, 458–476.

Carr, Peter and Sergey Nadtochiy. 2017. Local variance gamma and explicit calibration to option prices. *Mathematical Finance* 27(1), 151–193.

Corbetta, Jacopo, Pierre Cohort, Ismail Laachir, and Claude Martini. 2019. Robust calibration and arbitrage-free interpolation of ssvi slices. *Decisions in Economics and Finance* 42(2), 665–677.

De Boor, Carl. 1978. *A practical guide to splines*, Volume 27. Springer-Verlag New York.

Dupire, Bruno. 1994. Pricing with a smile. *Risk* 7(1), 18–20.

Falck, Markus and Mikhail Vladimirovich Deryabin. 2017. Local variance gamma revisited. *Available at SSRN 2659728*.

Gatheral, Jim. 2006. *The volatility surface: a practitioner's guide*, Volume 357. Wiley. com.

Hagan, Patrick S, Deep Kumar, Andrew S Lesniewski, and Diana E Woodward. 2002. Managing smile risk. *Wilmott magazine*.

Healy, Jherek. 2019. *Applied Quantitative Finance for Equity Derivatives*. Lulu.com.

Jäckel, Peter. 2014. Clamping down on arbitrage. *Wilmott* 2014(71), 54–69.

Jäckel, Peter. 2015. Let's be rational.

Kahalé, Nabil. 2004. An arbitrage-free interpolation of volatilities. *Risk* 17(5), 102–106.

Kanzow, Christian, Nobuo Yamashita, and Masao Fukushima. 2004. Levenberg-marquardt methods for constrained nonlinear equations with strong local convergence properties. *J. Computational and Applied Mathematics* 172, 375–397.

Klare, Kenneth and Guthrie Miller. 2013. Gn—a simple and effective nonlinear least-squares algorithm for the open source literature.

Le Floc'h, Fabien. 2017. When SVI breaks down. <https://chasethedevil.github.io/post/when-svi-breaks-down>.

Le Floc'h, Fabien. 2021. An arbitrage-free interpolation of class \mathcal{C}^2 for option prices. *The Journal of Derivatives* 28(4), 64–86.

Le Floc'h, Fabien and Cornelis W Oosterlee. 2019a. Model-free stochastic collocation for an arbitrage-free implied volatility: Part i. *Decisions in Economics and Finance* 42(2), 679–714.

Le Floc'h, Fabien and Cornelis W Oosterlee. 2019b. Model-free stochastic collocation for an arbitrage-free implied volatility, part ii. *Risks* 7(1), 30.

Wystup, Uwe. 2018. Arbitrage in the perfect volatility surface. *Wilmott* 2018(97), 16–17.

Appendix A Avoiding the use of complex numbers

We have $\chi_i = \sqrt{\frac{a(x)}{\alpha_i}}$ and we know that $a(x) \geq 0$ since all the B-spline coefficients are positive, thus χ_i is either real or imaginary if the sign of α_i is positive (respectively strictly negative). Since $V(x)$ involves the ratio $\chi_i(x)/\chi_i(x_i)$, we may equivalently calculate χ_i via $\chi_i = \sqrt{\frac{a(x)}{|\alpha_i|}}$.

From its definition, we know that ω_i is real if $\delta_i T + 8 \geq 0$ and imaginary otherwise.

For z_i we need to consider the two cases where the roots $\tilde{x}_{i,1}, \tilde{x}_{i,2}$ are both real or both complex.

If they are real, we have $\frac{x - \tilde{x}_{i,1}}{x - \tilde{x}_{i,2}} = \frac{a(x)}{\alpha_i(x - \tilde{x}_{i,2})^2}$. We know that $a(x) \geq 0$ since the B-spline coefficients are all positive. If $\alpha_i > 0$ then z_i is real, otherwise $z_i = \ln \left| \frac{x - \tilde{x}_{i,1}}{x - \tilde{x}_{i,2}} \right| + i\pi$.

If the roots are complex with non null imaginary parts, $\tilde{x}_{i,1}, \tilde{x}_{i,2}$ are conjugates of each other. We may write $\tilde{x}_{i,1} = u + i\nu$ and $\tilde{x}_{i,2} = u - i\nu$ with $(u, \nu) \in \mathbb{R} \times \mathbb{R}^*$. We have then $\left| \frac{x - \tilde{x}_{i,1}}{x - \tilde{x}_{i,2}} \right| = \left| \frac{x - u - i\nu}{x - u + i\nu} \right| = 1$ and thus z_i is imaginary.

The term $\cosh(\omega_i(z_i(x) - z_i(x_i)))$ is thus always real. When $\omega_i(z_i(x) - z_i(x_i))$ is imaginary, the term $\sinh(\omega_i(z_i(x) - z_i(x_i)))$ is imaginary.

To evaluate the expression $V(x)$, there are three cases two consider:

- $\delta_i \geq 0$ and $\delta_i T + 8 \geq 0$. All the variables are real.
- $\delta_i < 0$ and $\delta_i T + 8 \geq 0$. The logarithm in z_i may be calculated using $\Im(z_i(x)) = \arcsin \left[\Im \left(\frac{x - \tilde{x}_{i,1}}{x - \tilde{x}_{i,2}} \right) \right]$. The imaginary part may be directly calculated (without complex numbers). Then use $\cos[\bar{\omega}_i \Im(z_i(x))]$, $\sin[-\bar{\omega}_i \Im(z_i(x))]$ instead of \cosh and \sinh terms. Θ_i^s will then be real instead of complex.
- $\delta_i < 0$ and $\delta_i T + 8 < 0$. The logarithm in z_i may be calculated using $\Im(z_i(x)) = \arcsin \left[\Im \left(\frac{x - \tilde{x}_{i,1}}{x - \tilde{x}_{i,2}} \right) \right]$. The imaginary part may be directly calculated (without complex numbers). Then use $\cosh[\bar{\omega}_i \Im(z_i(x))]$, $\sinh[-\bar{\omega}_i \Im(z_i(x))]$.

Appendix B Market data

Table A1. Implied volatilities SPX500 European options expiring on March 24, 2017 (one week, $T = 0.021918$) assuming proportional dividends, with $r = 0.9\%$ and implied forward $F(T) = 2385.103981$. y represents the log-moneyness $\ln \frac{K}{F}$ taken from [Le Floc'h \[2017\]](#), also in [Healy \[2019\]](#).

| Strike | y | Volume | Vol | Call Bid | Call Ask | Put Bid | Put Ask |
|--------|---------|--------|------|----------|----------|---------|---------|
| 1800 | -0.2815 | 0 | 0.58 | 0.00 | 1.24 | 0.00 | 0.61 |
| 1850 | -0.2541 | 3300 | 0.53 | 0.00 | 1.14 | 0.00 | 0.56 |
| 1875 | -0.2406 | 3402 | 0.50 | 0.00 | 1.09 | 0.00 | 0.53 |
| 1880 | -0.2380 | 1551 | 0.54 | 0.00 | 1.08 | 0.52 | 0.56 |
| 1890 | -0.2327 | 200 | 0.53 | 0.00 | 1.06 | 0.51 | 0.55 |
| 1900 | -0.2274 | 200 | 0.52 | 0.00 | 1.04 | 0.50 | 0.53 |
| 1910 | -0.2221 | 0 | 0.49 | 0.00 | 1.02 | 0.00 | 0.52 |
| 1980 | -0.1861 | 3 | 0.43 | 0.00 | 0.89 | 0.42 | 0.45 |
| 1990 | -0.1811 | 2 | 0.43 | 0.00 | 0.87 | 0.41 | 0.45 |
| 2000 | -0.1761 | 12 | 0.42 | 0.00 | 0.86 | 0.40 | 0.44 |
| 2010 | -0.1711 | 1 | 0.41 | 0.00 | 0.84 | 0.39 | 0.43 |
| 2030 | -0.1612 | 11 | 0.39 | 0.00 | 0.80 | 0.37 | 0.41 |
| 2035 | -0.1587 | 1 | 0.38 | 0.00 | 0.79 | 0.36 | 0.40 |
| 2050 | -0.1514 | 10 | 0.38 | 0.00 | 0.76 | 0.37 | 0.40 |
| 2055 | -0.1490 | 10 | 0.38 | 0.00 | 0.75 | 0.36 | 0.39 |
| 2085 | -0.1345 | 11 | 0.36 | 0.00 | 0.69 | 0.34 | 0.36 |
| 2090 | -0.1321 | 1 | 0.35 | 0.00 | 0.69 | 0.34 | 0.36 |
| 2100 | -0.1273 | 105 | 0.34 | 0.00 | 0.67 | 0.33 | 0.35 |
| 2105 | -0.1249 | 1 | 0.33 | 0.00 | 0.66 | 0.32 | 0.34 |
| 2120 | -0.1178 | 6 | 0.32 | 0.00 | 0.63 | 0.32 | 0.33 |
| 2125 | -0.1155 | 111 | 0.32 | 0.00 | 0.62 | 0.31 | 0.33 |
| 2130 | -0.1131 | 1 | 0.31 | 0.00 | 0.61 | 0.30 | 0.32 |
| 2135 | -0.1108 | 11 | 0.31 | 0.00 | 0.61 | 0.30 | 0.31 |
| 2140 | -0.1084 | 10 | 0.31 | 0.00 | 0.60 | 0.30 | 0.31 |
| 2150 | -0.1038 | 6610 | 0.29 | 0.00 | 0.53 | 0.29 | 0.30 |
| 2155 | -0.1015 | 1 | 0.29 | 0.00 | 0.52 | 0.28 | 0.30 |
| 2160 | -0.0991 | 8 | 0.29 | 0.00 | 0.51 | 0.28 | 0.30 |
| 2165 | -0.0968 | 2 | 0.28 | 0.00 | 0.50 | 0.28 | 0.29 |
| 2175 | -0.0922 | 3 | 0.27 | 0.00 | 0.48 | 0.27 | 0.28 |
| 2180 | -0.0899 | 66 | 0.27 | 0.00 | 0.47 | 0.27 | 0.28 |
| 2185 | -0.0876 | 15 | 0.27 | 0.00 | 0.46 | 0.26 | 0.27 |
| 2190 | -0.0853 | 26 | 0.26 | 0.00 | 0.45 | 0.26 | 0.27 |
| 2195 | -0.0831 | 13 | 0.26 | 0.00 | 0.44 | 0.25 | 0.26 |
| 2200 | -0.0808 | 113 | 0.25 | 0.00 | 0.43 | 0.25 | 0.25 |
| 2205 | -0.0785 | 13 | 0.25 | 0.00 | 0.42 | 0.25 | 0.25 |
| 2210 | -0.0762 | 14 | 0.24 | 0.00 | 0.41 | 0.24 | 0.25 |
| 2215 | -0.0740 | 102 | 0.24 | 0.00 | 0.41 | 0.23 | 0.24 |
| 2220 | -0.0717 | 2 | 0.23 | 0.00 | 0.40 | 0.23 | 0.24 |
| 2225 | -0.0695 | 43 | 0.23 | 0.00 | 0.39 | 0.22 | 0.23 |
| 2230 | -0.0672 | 93 | 0.22 | 0.00 | 0.38 | 0.22 | 0.23 |
| 2235 | -0.0650 | 2 | 0.22 | 0.00 | 0.37 | 0.21 | 0.22 |
| 2240 | -0.0628 | 134 | 0.21 | 0.00 | 0.36 | 0.21 | 0.22 |
| 2245 | -0.0605 | 11 | 0.21 | 0.00 | 0.35 | 0.21 | 0.21 |
| 2250 | -0.0583 | 104 | 0.20 | 0.00 | 0.34 | 0.20 | 0.21 |
| 2255 | -0.0561 | 205 | 0.20 | 0.00 | 0.34 | 0.20 | 0.20 |
| 2260 | -0.0539 | 184 | 0.19 | 0.00 | 0.33 | 0.19 | 0.20 |
| 2265 | -0.0517 | 89 | 0.19 | 0.00 | 0.32 | 0.19 | 0.19 |
| 2270 | -0.0495 | 74 | 0.18 | 0.00 | 0.28 | 0.18 | 0.19 |
| 2275 | -0.0473 | 377 | 0.18 | 0.00 | 0.27 | 0.18 | 0.18 |
| 2280 | -0.0451 | 207 | 0.17 | 0.00 | 0.26 | 0.17 | 0.17 |
| 2285 | -0.0429 | 478 | 0.17 | 0.00 | 0.25 | 0.17 | 0.17 |
| 2290 | -0.0407 | 295 | 0.16 | 0.00 | 0.24 | 0.16 | 0.17 |
| 2295 | -0.0385 | 280 | 0.16 | 0.00 | 0.18 | 0.16 | 0.16 |
| 2300 | -0.0363 | 1106 | 0.15 | 0.00 | 0.18 | 0.15 | 0.16 |
| 2305 | -0.0342 | 377 | 0.15 | 0.00 | 0.17 | 0.15 | 0.15 |
| 2310 | -0.0320 | 793 | 0.14 | 0.00 | 0.17 | 0.14 | 0.15 |
| 2315 | -0.0298 | 567 | 0.14 | 0.09 | 0.16 | 0.14 | 0.14 |
| 2320 | -0.0277 | 864 | 0.14 | 0.09 | 0.15 | 0.13 | 0.14 |
| 2325 | -0.0255 | 569 | 0.13 | 0.10 | 0.15 | 0.13 | 0.13 |
| 2330 | -0.0234 | 567 | 0.13 | 0.10 | 0.14 | 0.13 | 0.13 |
| 2335 | -0.0212 | 260 | 0.12 | 0.10 | 0.14 | 0.12 | 0.12 |
| 2340 | -0.0191 | 407 | 0.12 | 0.10 | 0.13 | 0.12 | 0.12 |
| 2345 | -0.0170 | 506 | 0.12 | 0.10 | 0.13 | 0.11 | 0.12 |
| 2350 | -0.0148 | 1850 | 0.11 | 0.10 | 0.12 | 0.11 | 0.11 |
| 2355 | -0.0127 | 528 | 0.11 | 0.10 | 0.11 | 0.11 | 0.11 |
| 2360 | -0.0106 | 1134 | 0.10 | 0.10 | 0.11 | 0.10 | 0.11 |
| 2365 | -0.0085 | 436 | 0.10 | 0.10 | 0.10 | 0.10 | 0.10 |
| 2370 | -0.0064 | 1063 | 0.10 | 0.09 | 0.10 | 0.10 | 0.10 |

| | | | | | | | |
|------|---------|------|------|------|------|------|------|
| 2375 | -0.0042 | 1420 | 0.09 | 0.09 | 0.10 | 0.09 | 0.10 |
| 2380 | -0.0021 | 1248 | 0.09 | 0.09 | 0.09 | 0.09 | 0.09 |
| 2385 | 0.0000 | 229 | 0.09 | 0.09 | 0.09 | 0.09 | 0.09 |
| 2390 | 0.0021 | 2252 | 0.09 | 0.09 | 0.09 | 0.09 | 0.09 |
| 2395 | 0.0041 | 912 | 0.09 | 0.09 | 0.09 | 0.08 | 0.09 |
| 2400 | 0.0062 | 2650 | 0.09 | 0.08 | 0.09 | 0.08 | 0.09 |
| 2405 | 0.0083 | 2523 | 0.08 | 0.08 | 0.09 | 0.08 | 0.09 |
| 2410 | 0.0104 | 789 | 0.08 | 0.08 | 0.09 | 0.08 | 0.10 |
| 2415 | 0.0125 | 863 | 0.08 | 0.08 | 0.08 | 0.07 | 0.10 |
| 2420 | 0.0145 | 905 | 0.08 | 0.08 | 0.09 | 0.00 | 0.13 |
| 2425 | 0.0166 | 1178 | 0.09 | 0.08 | 0.09 | 0.00 | 0.13 |
| 2430 | 0.0187 | 815 | 0.09 | 0.08 | 0.09 | 0.00 | 0.14 |
| 2435 | 0.0207 | 267 | 0.09 | 0.09 | 0.09 | 0.00 | 0.15 |
| 2440 | 0.0228 | 402 | 0.09 | 0.09 | 0.09 | 0.00 | 0.16 |
| 2445 | 0.0248 | 50 | 0.09 | 0.09 | 0.09 | 0.00 | 0.17 |
| 2450 | 0.0268 | 2027 | 0.09 | 0.09 | 0.10 | 0.00 | 0.17 |
| 2455 | 0.0289 | 59 | 0.10 | 0.10 | 0.10 | 0.00 | 0.18 |
| 2460 | 0.0309 | 159 | 0.10 | 0.10 | 0.10 | 0.00 | 0.19 |
| 2465 | 0.0330 | 26 | 0.10 | 0.10 | 0.11 | 0.00 | 0.20 |
| 2470 | 0.0350 | 53 | 0.10 | 0.10 | 0.11 | 0.00 | 0.21 |
| 2475 | 0.0370 | 229 | 0.11 | 0.10 | 0.11 | 0.00 | 0.22 |
| 2495 | 0.0450 | 1 | 0.12 | 0.11 | 0.13 | 0.00 | 0.25 |
| 2550 | 0.0669 | 800 | 0.15 | 0.00 | 0.16 | 0.00 | 0.37 |

Table A2. Implied volatility quotes for SPX500 options expiring on March 7, 2018, as of February, 5, 2018. In ACT/365, the option maturity is $T = 0.082192$. The implied forward price is $F(0, T) = 2629.80$. The interest rate is $r = 0.97\%$.

| Strike | Logmoneyness | Implied vol. | Strike | Logmoneyness | Implied vol. |
|--------|--------------|--------------|--------|--------------|--------------|
| 1900 | -0.325055 | 0.684883 | 2650 | 0.007651 | 0.280853 |
| 1950 | -0.299079 | 0.6548 | 2655 | 0.009536 | 0.277035 |
| 2000 | -0.273762 | 0.627972 | 2660 | 0.011417 | 0.273715 |
| 2050 | -0.249069 | 0.604067 | 2665 | 0.013295 | 0.270891 |
| 2100 | -0.224971 | 0.576923 | 2670 | 0.01517 | 0.267889 |
| 2150 | -0.201441 | 0.551253 | 2675 | 0.017041 | 0.264533 |
| 2200 | -0.178451 | 0.526025 | 2680 | 0.018908 | 0.262344 |
| 2250 | -0.155979 | 0.500435 | 2685 | 0.020772 | 0.258598 |
| 2300 | -0.134 | 0.474137 | 2690 | 0.022632 | 0.2555 |
| 2325 | -0.123189 | 0.461716 | 2695 | 0.024489 | 0.25219 |
| 2350 | -0.112493 | 0.445709 | 2700 | 0.026343 | 0.249534 |
| 2375 | -0.101911 | 0.433661 | 2705 | 0.028193 | 0.246659 |
| 2400 | -0.09144 | 0.42016 | 2710 | 0.03004 | 0.243553 |
| 2425 | -0.081077 | 0.407463 | 2715 | 0.031883 | 0.240202 |
| 2450 | -0.070821 | 0.393168 | 2720 | 0.033723 | 0.236588 |
| 2470 | -0.062691 | 0.381405 | 2725 | 0.03556 | 0.234574 |
| 2475 | -0.060668 | 0.3793 | 2730 | 0.037393 | 0.230407 |
| 2480 | -0.05865 | 0.377109 | 2735 | 0.039223 | 0.227866 |
| 2490 | -0.054626 | 0.372471 | 2740 | 0.041049 | 0.223049 |
| 2510 | -0.046626 | 0.360294 | 2745 | 0.042872 | 0.219888 |
| 2520 | -0.04265 | 0.354671 | 2750 | 0.044692 | 0.218498 |
| 2530 | -0.03869 | 0.350533 | 2755 | 0.046509 | 0.214702 |
| 2540 | -0.034745 | 0.344119 | 2760 | 0.048322 | 0.210506 |
| 2550 | -0.030815 | 0.339273 | 2765 | 0.050132 | 0.208175 |
| 2560 | -0.026902 | 0.333069 | 2770 | 0.051939 | 0.205508 |
| 2570 | -0.023003 | 0.328206 | 2775 | 0.053742 | 0.199967 |
| 2575 | -0.021059 | 0.324314 | 2780 | 0.055542 | 0.199007 |
| 2580 | -0.019119 | 0.322041 | 2785 | 0.057339 | 0.195062 |
| 2590 | -0.015251 | 0.3168 | 2790 | 0.059133 | 0.190547 |
| 2600 | -0.011397 | 0.310914 | 2795 | 0.060923 | 0.188427 |
| 2610 | -0.007559 | 0.305042 | 2800 | 0.062711 | 0.185893 |
| 2615 | -0.005645 | 0.302416 | 2805 | 0.064495 | 0.182878 |
| 2620 | -0.003734 | 0.299488 | 2810 | 0.066276 | 0.179292 |
| 2625 | -0.001828 | 0.29609 | 2815 | 0.068053 | 0.175001 |
| 2630 | 7.5E-05 | 0.292378 | 2835 | 0.075133 | 0.185751 |
| 2635 | 0.001974 | 0.289516 | 2860 | 0.083913 | 0.207173 |
| 2640 | 0.00387 | 0.28584 | 2900 | 0.097802 | 0.225248 |
| 2645 | 0.005762 | 0.283342 | | | |

Table A3. Implied volatilities of TSLA American options expiring on March 21, 2025 as of February, 21 2025 ($T = 0.076712$) with implied spot $S = 351.9764$ and forward $F(T) = 353.4459$, a discount rate $r = 4.38987\%$.

| Call | | | Put | | |
|--------|-----------|----------|--------|-----------|----------|
| Strike | Mid Price | Vol in % | Strike | Mid Price | Vol in % |
| 355 | 18.725 | 50.00 | 90 | 0.050 | 172.19 |
| 365 | 14.600 | 50.17 | 100 | 0.070 | 164.49 |
| 375 | 11.275 | 50.49 | 125 | 0.085 | 139.13 |
| 380 | 9.875 | 50.68 | 135 | 0.090 | 130.07 |
| 385 | 8.625 | 50.86 | 140 | 0.105 | 127.45 |
| 395 | 6.575 | 51.38 | 150 | 0.125 | 120.75 |
| 400 | 5.725 | 51.63 | 155 | 0.140 | 117.89 |
| 410 | 4.350 | 52.26 | 160 | 0.160 | 115.39 |
| 415 | 3.800 | 52.63 | 165 | 0.175 | 112.39 |

| | | | | | |
|-----|-------|-------|-----|--------|--------|
| 440 | 2.020 | 55.04 | 170 | 0.195 | 109.71 |
| 445 | 1.795 | 55.58 | 180 | 0.235 | 104.16 |
| 450 | 1.600 | 56.15 | 190 | 0.275 | 98.47 |
| 455 | 1.440 | 56.80 | 195 | 0.295 | 95.61 |
| 465 | 1.170 | 58.07 | 200 | 0.315 | 92.73 |
| 470 | 1.060 | 58.72 | 210 | 0.360 | 87.15 |
| 490 | 0.735 | 61.38 | 215 | 0.380 | 84.26 |
| 500 | 0.625 | 62.78 | 220 | 0.405 | 81.53 |
| 505 | 0.575 | 63.42 | 225 | 0.430 | 78.79 |
| 510 | 0.535 | 64.14 | 230 | 0.460 | 76.17 |
| 520 | 0.460 | 65.46 | 240 | 0.525 | 70.98 |
| 525 | 0.425 | 66.05 | 250 | 0.635 | 66.51 |
| 545 | 0.325 | 68.68 | 255 | 0.700 | 64.32 |
| 550 | 0.305 | 69.32 | 260 | 0.785 | 62.33 |
| 560 | 0.270 | 70.60 | 265 | 0.890 | 60.47 |
| 565 | 0.255 | 71.25 | 270 | 1.030 | 58.85 |
| 575 | 0.225 | 72.40 | 285 | 1.685 | 54.74 |
| 580 | 0.210 | 72.90 | 290 | 2.025 | 53.69 |
| 625 | 0.135 | 78.29 | 295 | 2.455 | 52.81 |
| 630 | 0.130 | 78.92 | 300 | 2.975 | 52.00 |
| 640 | 0.120 | 80.11 | 305 | 3.650 | 51.49 |
| 645 | 0.120 | 81.02 | 310 | 4.425 | 50.90 |
| 650 | 0.110 | 81.20 | 325 | 7.850 | 50.05 |
| 655 | 0.100 | 81.30 | 330 | 9.400 | 49.96 |
| 660 | 0.095 | 81.76 | 350 | 17.750 | 49.96 |
| 700 | 0.065 | 85.33 | | | |
| 710 | 0.055 | 85.59 | | | |
| 720 | 0.050 | 86.37 | | | |
| 730 | 0.045 | 87.05 | | | |
| 750 | 0.035 | 88.03 | | | |
| 770 | 0.030 | 89.63 | | | |
| 800 | 0.030 | 93.53 | | | |
| 810 | 0.020 | 91.87 | | | |
| 820 | 0.020 | 93.08 | | | |

Table A4. Quotes for options on AUD/NZD currency pair of maturity July 9th, 2014 as of July 2nd, 2014.
 $S = 1.0784$, $F(0, T) = 1.07845$, $B(0, T) = 0.999712587139$, 10Δ RR = 0.35%, 25Δ RR = 0.40%, ATM vol = 5.14%,
 25Δ BF = 0.25%, 10Δ BF = 1.175%.

| Maturity | 10 Δ -Put | 25 Δ -Put | ATM | 25 Δ -Call | 10 Δ -Call |
|----------|------------------|------------------|-------|-------------------|-------------------|
| 1w | 6.14% | 5.19% | 5.14% | 5.59% | 6.49% |

Table A5. Black-Scholes implied volatilities against moneyness $\frac{x}{X(0)}$ for an option of maturity $T = 5.0722$, examples 1 and 2 of [Jäckel 2014].

| Moneyness | Volatility (Case I) | Volatility (Case II) |
|-------------------|---------------------|----------------------|
| 0.035123777453185 | 0.642412798191439 | 0.649712512502887 |
| 0.049095433048156 | 0.621682849924325 | 0.629372247414191 |
| 0.068624781300891 | 0.590577891369241 | 0.598339248024188 |
| 0.095922580089594 | 0.553137221952525 | 0.560748840467284 |
| 0.134078990076508 | 0.511398042127817 | 0.518685454812697 |
| 0.18741338653678 | 0.466699250819768 | 0.473512707134552 |
| 0.261963320525776 | 0.420225808661573 | 0.426434688827871 |
| 0.366167980681693 | 0.373296313420122 | 0.378806875802102 |
| 0.511823524787378 | 0.327557513727855 | 0.332366264644264 |
| 0.715418426368358 | 0.285106482185545 | 0.289407658380454 |
| 1 | 0.24932882881654 | 0.253751752243855 |
| 1.39778339939642 | 0.228967051575314 | 0.235378088110653 |
| 1.95379843162821 | 0.220857187809035 | 0.235343538571543 |
| 2.73098701349666 | 0.218762825294675 | 0.260395028879884 |
| 3.81732831143284 | 0.218742183617652 | 0.31735041252779 |
| 5.33579814376678 | 0.218432406892364 | 0.368205175099723 |
| 7.45829006788743 | 0.217198426268117 | 0.417582432865276 |
| 10.4250740447762 | 0.21573928902421 | 0.46323707706565 |
| 14.5719954372667 | 0.214619929462215 | 0.504386489988866 |
| 20.3684933182917 | 0.2141074555437 | 0.539752566560924 |
| 28.4707418310251 | 0.21457985392644 | 0.566370957381163 |